



Convection Enhancement Using Composite Vortex Generator

S. A. Gandjalikhan Nassab*, M. Moein Addini

Department of Mechanical Engineering, Shahid Bahonar University of Kerman, Kerman, Iran

ABSTRACT: This paper presents an original concept of using a composite flexible flapping vortex generator mounted on a heat sink fin for air side heat transfer augmentation. The main aim is to combine the advantages of hard and soft winglets in a composite one for having the highest possible enhancement. The proposed composite vortex generator, which is made with a thin elastic sheet is responsible for enhancing heat transfer and mixing quality performances in laminar convection air flow in a heat sink. The merged vortical structures due to oscillation by winglet swept out the thermal boundary layer and enhance thermal mixing between the fluid near the heated fin and the channel core flow. This novel concept is demonstrated using numerical simulation of the flow field with considering a two-way strongly coupled fluid-solid interaction approach in transient condition. The set of governing equations including, the continuity, momentum, and energy for a 2-D forced convection air flow are solved by the finite element method using the COMSOL Multi-Physics. The present findings show 148%, 116%, and 121% increases in the cooling rate by the composite and the two hard and soft homogeneous winglets, respectively. Numerical results are validated against the numerical data reported in the literature.

Review History:

Received: Jun. 09, 2021
Revised: Aug. 29, 2021
Accepted: Oct. 09, 2021
Available Online: Oct. 12, 2021

Keywords:

Convection augmentation
Composite vortex generator
Flapping mode
Heat sink

1- Introduction

In recent years, several countries have experienced limited freshwater because of the fast growing of population. Increasing the dry cooling in many thermal systems such as heat exchangers could save a considerable amount of freshwater. On the other hand, the airside convective heat transfer coefficient is about two orders of magnitude lower than that for water and dry cooling or heating require a much higher pumping power and heat exchanger surface to transfer the same amount of heat.

Much attention has been focused on this subject by many researchers up to now. The vortex generation technique is one of the efficient methods for heat transfer augmentation, and different types of Vortex Generators (VGs) have been investigated up to now. Two main categories are stationary and vibrating vortex generators. Also, two ways exist to fulfill the oscillating vortex generators; the active method with external power and the passive method with Fluid-Structure Interaction (FSI). The present work focuses on the passive VGs that have been employed to enhance heat transfer in different applications. Recently, the Fluid-Solid Interaction (FSI) has been a topic of many research works [1, 2], and it was shown that the generated flow vortices by the oscillating VG cause flow mixing by breaking the thermal boundary layer that finally leads to heat transfer augmentation in convective flows.

In the passive vortex generation technique, elastic structures are placed between the airside heat exchanger fins for

heat transfer enhancement. Vibrating micro fin array located on the fin has been discussed by Go [3] for heat transfer enhancement in laminar air convection flow, and a 10% increase in the rate of heat transfer was reported due to VG at the same velocity. Mounting multiple elastic structures on the fin has been discussed by others [4, 5], and more rate of convection heat transfer than the single VG was reported. The thermal performance related to the material properties has been studied for flapping vortex generators by Li et al. [6]. Three flapping vortex generators with different stiffness were compared for airside heat transfer enhancement. The proposed vortex generator was made with a thin elastic sheet bonded to the inner wall of the heat sink channel. The main focus was on the effects of Young's Modulus on the heat transfer performances by the vortex generator. In that study, the flow equations and the equation that governs the VG vibration were solved by the Finite Volume Method (FVM) using the COMSOL Multi-Physics. Numerical results demonstrated that the vortex generator with a Young's Modulus of 1 MPa has the best performance among the other three choices and can enhance the rejected heat by 140% at the same velocity and 87% at the same total pumping power.

The effect of self-sustained passive oscillations of multiple flags in a two-dimensional laminar flow on heat transfer enhancement was studied numerically by Ali et al. [7]. The flexible flags were located on two opposite channel walls in different alternating positions. To solve the set of governing equations, the two-way strongly-coupled FSI simulations

*Corresponding author's email: ganj110@uk.ac.ir



were performed by coupling ANSYS Fluent (Computational Fluid Dynamics (CFD) solver) with ANSYS Mechanical (Computational Structural Dynamics (CSD) solver). Five test cases were analyzed, and they differ by the number of alternating flaps and by the presence or absence of two coplanar flaps at the upstream. Numerical results showed that mixing is enhanced for larger flaps displacement achieving up to 99% in mixing homogeneity. Moreover, the high amplitude oscillations, when compared to the results of a clean channel, showed a great ability to reduce the thickness of the thermal boundary layer and to enhance heat transfer resulting in up to 275% increase in the global Nusselt number on the heated walls.

The heat transfer performance of flag vortex generators in rectangular channels was studied experimentally by Gallegos and Sharma [8]. In that experimental work, the heat transfer characteristic of turbulent convection airflow under the presence of a flapping flag as a VG was investigated. Also, the influences of channel geometry, flag material properties, and flow conditions on the resulting heat transfer behavior of the system were thoroughly explored. As an important finding, it was revealed that the inclusion of a flapping flag in the channel enhances the flow instability and turbulence levels, leading to Nusselt number enhancement by as high as 1.34 to 1.62 times bare channel levels. The heat transfer enhancement by flexible winglets clamped vertically in a Poiseuille channel flow was studied by Lee et al. [9]. The penalty immersed boundary method was adopted to analyze the FSI between the surrounding fluid and the flexible flags. It was seen that the VGs display three distinct movement modes: a flapping mode, a fully deflected mode, and an irregular mode depending on the relationship between the hydrodynamic force and the restoring force.

A two-dimensional numerical simulation was performed by Park [10], to examine the effects of the self-sustained oscillating motion of VGs on heat transfer. The wall-mounted flexible flag with an inclination angle was used to promote the fluid mixing and increase the heat transfer without much increasing the energy loss. The fluid-flexible body-thermal interaction was considered on the framework of the immersed boundary method. As the main result, it was observed that the rate of heat transfer is significantly increased due to the vortex merging process when the oscillation of VG takes place at the flapping mode.

For convection enhancement utilizing the vortex generation technique, it is clear that the frequency and amplitude of vibration are much affected by the rigidity factor of vibrators. Winglets made with hard material oscillate with small amplitude and high frequency, and the opposite behavior occurs

in soft winglets [9]. To gather both advantages of high frequency and amplitude, which are responsible for a considerable mixing rate, the author proposed using composite vortex generators. To materialize this aim, three different test cases, including homogenous and composite VGs inside a 2-D laminar convection air flow in a heat sink with constant fin temperature, were simulated. The test cases include two homogeneous VGs and one composite VG for comparing their performances. The soft and hard homogeneous VGs have the module of elasticities $E=0.01$ MPa and 0.1 MPa, respectively, and for the composite winglet, the first part attached to the fin is made with hard material ($E=0.1$ MPa) and the second part is soft ($E=0.01$ MPa). In the numerical simulation, a comprehensive transient thermo hydrodynamic analysis is done by the solution of continuity, momentum, and energy equations considering a two-way strongly-coupled FSI approach in transient condition by the Finite Element Analysis (FEM). Besides, to show the positive effect of composite flexible VG and its pros and cons, extensive comparisons were made with its original version; the homogenous vortex generator and the conventional clean heat sink.

2- Theory

A schematic diagram of the computational domain and the coordinate system is shown in Fig. 1. The length of the flexible thin elastic sheet attached to the lower fin surface is defined by L_{VG} . The leading edge of VG is clamped at the bottom wall, and the trailing edge is free with the inclination angle $\beta = 80^\circ$. The position of the clamped leading edge from the inlet is denoted by x_0 , equals to 0.5 m. The channel height and length are $H=0.4$ m and $L=2.5$ m, respectively. The laminar air flow enters between two heated fins with a fully developed velocity profile and a maximum velocity of 0.4 m/s. The regime of convective flow is laminar because the value of Reynolds number defined as $\rho \bar{V} D_h / \mu$ becomes equal to 2100 . At the inlet section, the air flow temperature is $T_{in} = 293$ K and the fin surfaces are at $T_w = 430$ K. In the simulation, all of the air thermo-physical properties are considered temperature dependent, because of the large temperature difference between the inlet air and the heated walls. The VG information is also reported in Table. 1.

In the case of homogenous VGs, the module of elasticities are 0.1 MPa, and 0.01 MPa corresponds to hard and soft winglets. For composite VG, the value of Young's modulus is varied along with the winglet as shown in Fig. 2. It is worth mentioning that the hard part of the VG causes vibration with high frequency, and the soft part at the top is responsible for generating high amplitude for the vibration of the composite winglet.

Table 1. VG information and characteristic

Length	Thickness	Attacked angle	Module of elasticity	Poison ratio	Density
18 mm	10 mm	82°	0.01-0.1 MPa	0.4	1000 kg/m^3

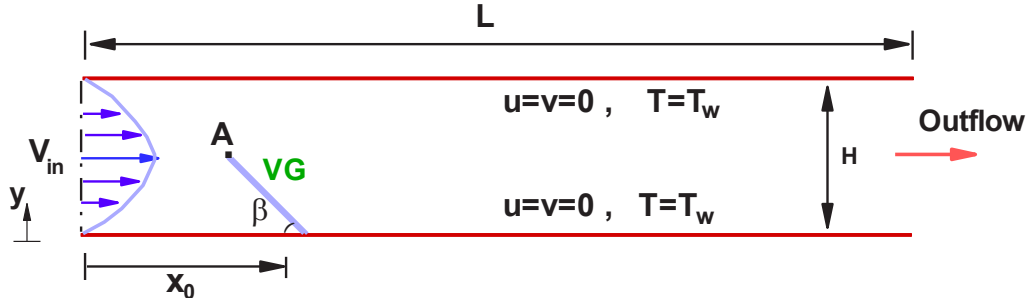


Fig. 1. Geometry definition and dimensions (point A is on the tip of VG)

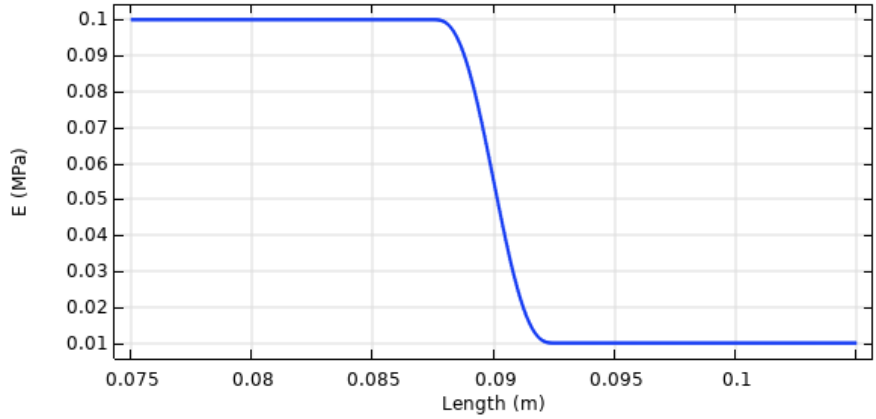
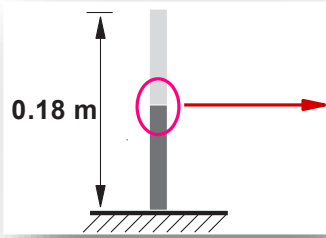


Fig. 2. Young modulus variation along the composite winglet

2- 1- Governing equations

The set of governing equations for transient Newtonian incompressible laminar air flow consists of conservation of mass, momentum, and energy coupled with VG vibration through the Fluid-Solid Interaction is as follows:

Continuity:

$$\frac{\partial u}{\partial x} + \frac{\partial v}{\partial y} = 0 \quad (1)$$

x-momentum:

$$\rho \left(\frac{\partial u}{\partial t} + u \frac{\partial u}{\partial x} + v \frac{\partial u}{\partial y} \right) = - \frac{\partial P}{\partial x} + \mu \nabla^2 u + F_{ext,x} \quad (2)$$

y-momentum:

$$\rho \left(\frac{\partial v}{\partial t} + u \frac{\partial v}{\partial x} + v \frac{\partial v}{\partial y} \right) = - \frac{\partial P}{\partial y} + \mu \nabla^2 v + F_{ext,y} \quad (3)$$

Energy:

$$\frac{\partial T}{\partial t} + u \frac{\partial T}{\partial x} + v \frac{\partial T}{\partial y} = \alpha \nabla^2 T \quad (4)$$

In momentum equations, F_{ext} is the external force on fluid due to transient vibration of elastic vortex generator. The flapping winglet not only experiences large deformations due to the receiving momentum from convective flow but also its vibration exerts a surface force on working gas as well. This situation is an interdisciplinary subject which is called two-way modeling in computational fluid dynamics [11]. The complete formulation of FSI that leads to form $F_{ext, VG}$ is provided by COMSOL Multiphysics Inc. [12] and Ref. [13].

The equation of motion for computing the oscillation of 2-D flapping VG exposed to the convection air flow can be written as [6]:

$$(\lambda + \mu_s) \frac{\partial}{\partial x_i} \left(\frac{\partial U_{sj}}{\partial x_i} \right) + \mu_s \frac{\partial}{\partial x_j} \left(\frac{\partial U_{si}}{\partial x_j} \right) = \rho_s \ddot{U}_{si}$$

Where, U_{si} is the displacement vector of the solid element. More details about the equation govern to the displacement of elastic winglets were given in the paper by Li et al. [6].

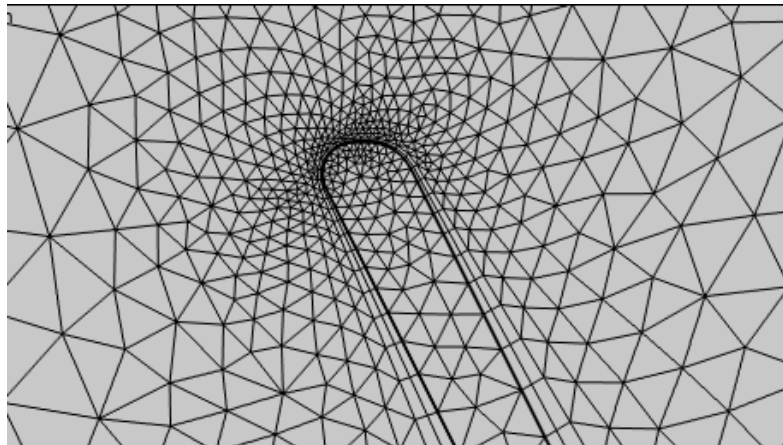
2- 2- Boundary conditions

In the numerical simulation of convection flow and the motion of VG, the following initial and boundary conditions are imposed:

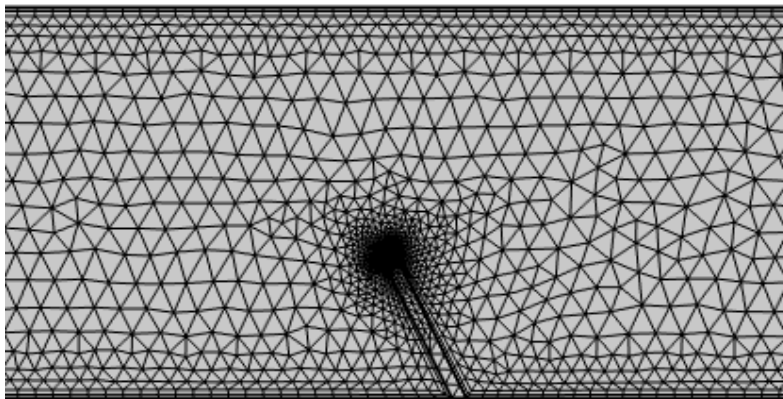
- At $t=0$, the air is stagnant, and its temperature equals to the ambient temperature (293 K).
- No-slip condition for all solid walls is employed in velocity computation and based on the continuity of temperature, the air temperature equals to $T_w = 430$ K.
- At the inlet section, the air flow has a fully developed velocity profile with a maximum velocity of 0.4 m/s and a uniform temperature of 293 K.
- Zero pressure is considered for the convective flow at the outlet section, and the gas temperature is corrected via the energy balance during the iterative procedure. Also, zero axial gradients are employed for the flow variables.

3- Mesh

Although the heat sink channel has a rectangular shape and the mapped mesh is the best choice for discretization, but the unstructured triangular grid generation method was used for the 2D geometry of the channel because of the inclined VG. Near the walls, the mesh was refined to precisely capture the high gradient of dependent variables, especially around the vibrating winglet (Fig. 3). A grid study was done to find an optimum number of grid nodes that makes numerical results reliable and independent from the spatial discretization and simultaneously confers a computationally cost-effective mesh. The results are tabulated in Table. 2, and the average values of the Nusselt number on the lower wall are reported at different mesh sizes. As seen, the relative error of sought parameter with respect to the previous step ($\Delta Nu / Nu_{previous\ grid}$) goes down as the number of nodes increases, such that at 12440 nodes, relative error falls below 1%. Fig. 4 also shows this fact and the trend of the average Nusselt number with the number of elements. Hence, the adopted mesh has 12440 nodes with an average element's quality of 0.9 and skewness of 0.45.



(a): High enlarged discretized domain



(b): Grids near VG and boundary walls

Fig. 3. The unstructured triangular mesh

Table 2. Effect of grid size on the converged solution

	Mesh-1	Mesh-2	Mesh-3	Mesh-4	Mesh-5
Number of node	5340	8500	10876	12440	14470
Average Nu	45.1	48.6	49.6	50.1	50.4
Error respect to the previous step	-	7.6%	2.1%	1.2%	0.5%

4- Method of Solution

The deformable elastic winglet inside the convective air flow experiences not only large deformations due to the receiving momentum from moving fluid but also its transient oscillations interact with surrounding continuous media, such that its reaction exerts a surface force on fluid as well. So, due to VG vibration, the computational domain including the flow field was considered the deforming region, and the continuity, momentum, and energy equations were solved with the moving mesh technique. The FEM was employed in the numerical solution of the governing equations, using the second order of discretizations in pressure, velocity, and temperature calculations. All of the computations were carried out using a computer with Intel(R) Core (TM) i5-3210M CPU@2.50 GHz. Since the governing equations were solved iteratively at each time step, convergence criteria were needed to distinguish the converged solution. The minimum residuals as convergence criteria are 5×10^{-4} for mass and momentum, and 10^{-4} for energy conservation equations. Besides, the maximum time step of 0.006 sec was employed in time marching up to semi-steady condition, while the VG reached its flapping or irregular mode. Computational results showed that after $t=100$ s, the simulated thermal systems reach their final states both for the homogeneous and composite VGs.

5- Validation

For validating the present analysis, a laminar convection gas flow in a rectangular duct with a heated surface and under the presence of an installed VG on the lower wall was simulated, and numerical results were compared to the findings obtained by Li et al. [6]. The same mesh and configuration were adapted to the dimensions of geometry that were used in the numerical study of Ref. [6]. For validating the numerical scheme, the averaged values of the Nusselt number on the lower wall were calculated at different Reynolds numbers and VG's modulus of elasticities. The computed Nusselt number was defined based on the average heat transfer coefficient (= rejected heat divided by the logarithmic mean temperature difference) and the hydraulic duct diameter ($2 \times$ Height). In Fig. 5, the variations of the average Nusselt number on the bottom wall with Reynolds number at different values of Young's modulus are plotted. An increasing trend for convection coefficient is seen with the Reynolds number. A very good agreement was found between our FEM simulation and Li et al. [6]. Also, Fig. 5 shows that the value of the Nusselt number

is inversely proportional with the young modulus which varies from an infinite value corresponding to the rigid body to 1.0 MPa, corresponding to high-elastic material, which results in a better heat transfer enhancement. In Table. 3, the values of relative errors between the computed Nusselt numbers with those reported in Ref. [6] are given at different values of Young's modulus and the Reynolds number. As seen, all computations have relative errors of less than 3.5% that shows the consistency between the results. This consistency was expected because both the present simulation and the one which was done by Li et al. [6] are based on the finite element method and using the COMSOL Multi-physics. It should be recalled that the differences between these results may be due to different factors, such as the round of errors and also the rate of grid clustering near to the VG, and also the boundary walls, which was not mentioned in that study [6]. Because the winglet elasticity and also the Reynolds number have considerable effects on the flow field, having a very good agreement on a wide variety of VG's elasticity shows the reliability of all involved numerical procedures.

6- Results and Discussion

6- 1- Dynamics of the flexible VG

In this paper, the set of governing equations for the laminar convection flow coupled with the equation of VG movement based on the FSI are solved numerically. Generally, the flexible elastic sheet as VG displays three distinct movement modes: a flapping mode, a fully deflected mode, and an irregular mode. The dominant mode at any given time depends on the relationship between the hydrodynamic and restoring forces. The VG in the flapping mode displays a continuous and regular fluttering movement as desired in convection enhancement. In the fully deflected mode, the VG is initially deflected by the hydrodynamic force, after which it reached a stationary state that is out of our interest because of the small mixing rate. The VG in irregular mode displays irregular oscillating movement with high frequency. It should be mentioned that for having a higher rate of mixing and convection augmentation, the VG oscillation with high frequency and large amplitude is desired. The numerical findings reported in the literature have been predicted the high frequency and small amplitude for rigid winglets (high Young's modulus) and opposite behavior for soft ones due to FSI [9]. So, both positive factors in convection enhancement are the vibration of VGs with both high amplitude and frequency is not gath-

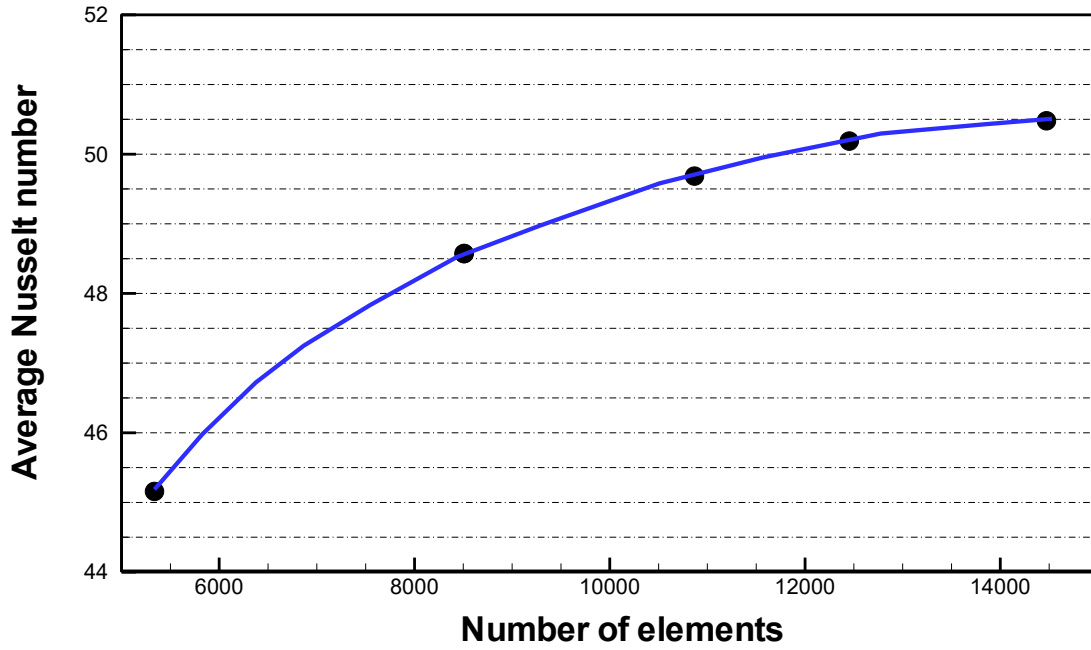


Fig. 4. Average Nusselt number on the lower wall at different number of grids

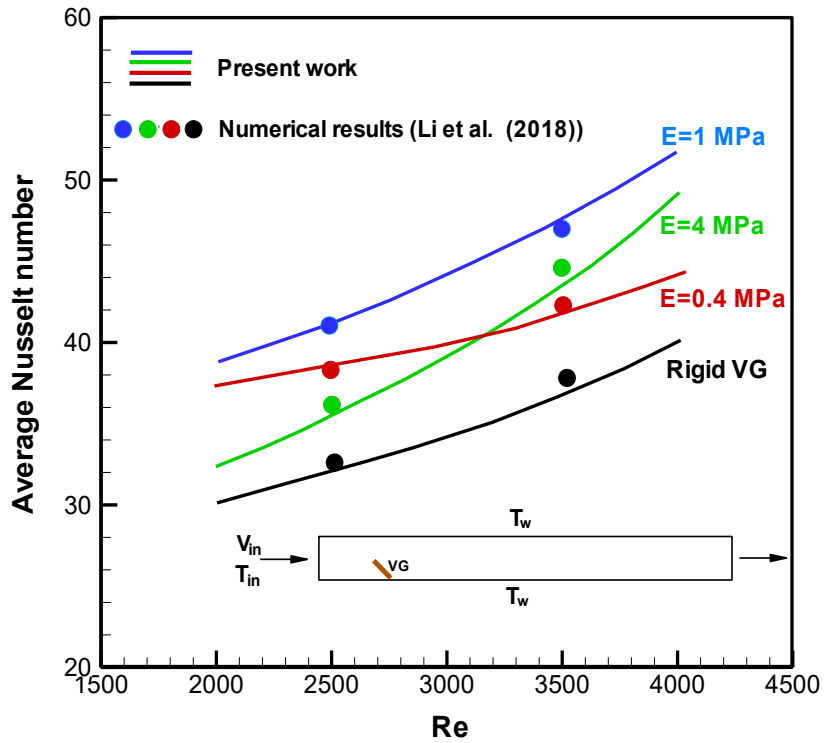
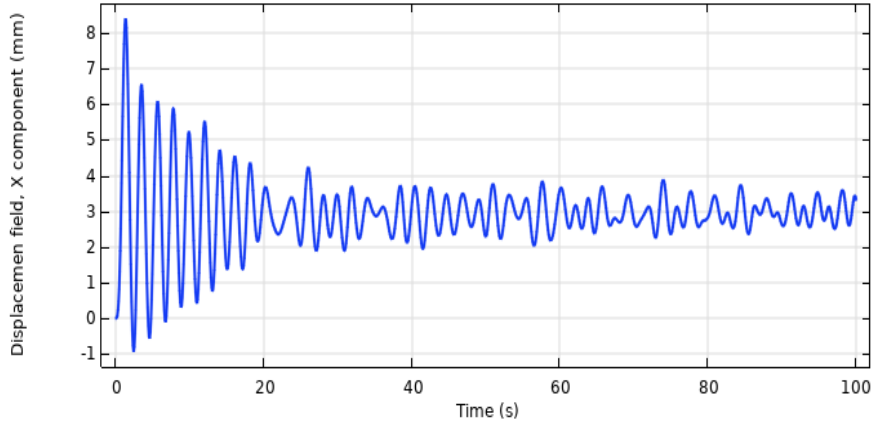
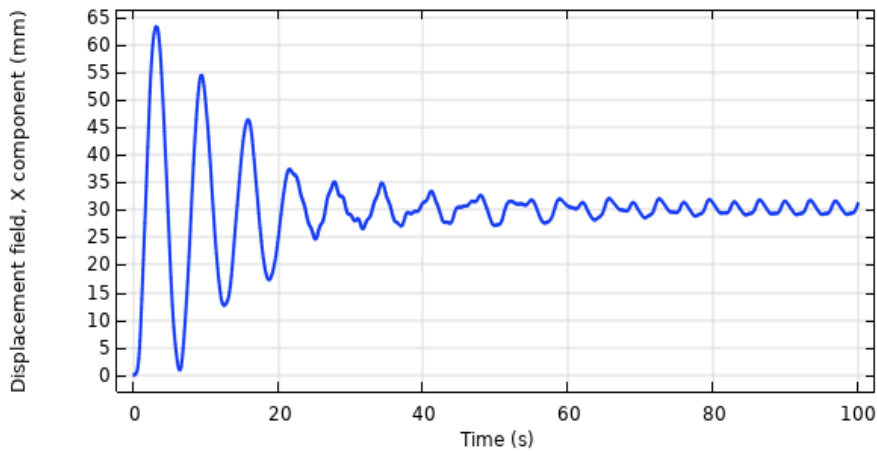


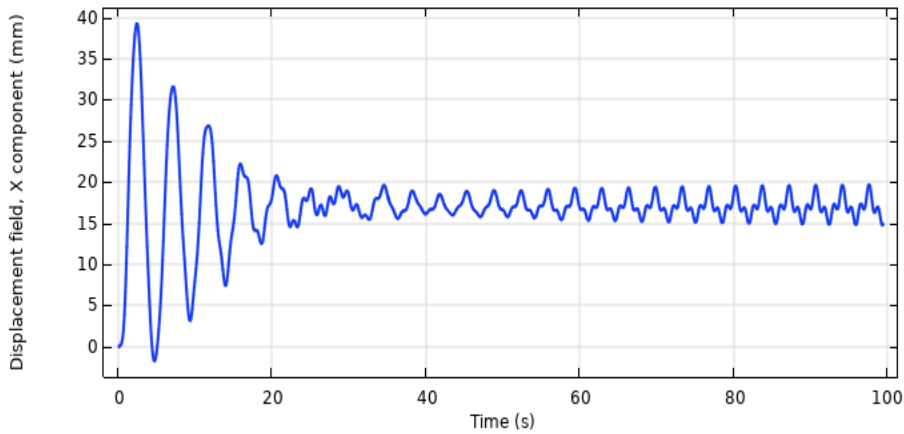
Fig. 5. Average Nusselt number on the lower wall for different values of Reynolds number and modulus of elasticity [6]



a) Homogeneous VG at irregular mode ($E=0.1$ MPa)



b) Homogeneous VG at flapping mode ($E=0.01$ MPa)



c) Composite VG at flapping mode

Fig. 6. Displacement of point A on the tip of VG

ered in a homogenous winglet. This fact motivates the author to use composite vortex generators. For comparing the behavior of homogeneous and composite winglets, the x-displacement of point A on the tip of VGs during the time period $0 \leq t \leq 100s$ is shown in Fig. 6. If one notices the displacement of hard homogeneous VG shown in Fig. 6-a, a periodic

deformation with large displacement is seen at the early time stage, after which it changes to an irregular motion with low amplitude and relatively high frequency, corresponding to the irregular mode of vibration. It is clear that the high frequency of vibrating VG enhances the flow mixing, but the small amplitude of oscillation has the opposite effect.

Table 3. The values of relative errors between the computed averaged Nu with Ref. [6]

Young's modulus	0.4 (MPa)		1 (MPa)		4 (MPa)		Rigid	
Reynolds number	2500	3500	2500	3500	2500	3500	2500	3500
Relative error	1.1%	1.5%	0.8%	1.4%	1.7%	3.2%	2.1%	3.4%

Table 4. Amplitudes and frequencies of VG at their semi-steady states

VG	Homog. ($E=0.01$ MPa)	Composite	Homog. ($E=0.1$ MPa)
Amplitude (mm)	3.5	5.1	0.9
Frequency (1/s)	0.30	0.28	0.61

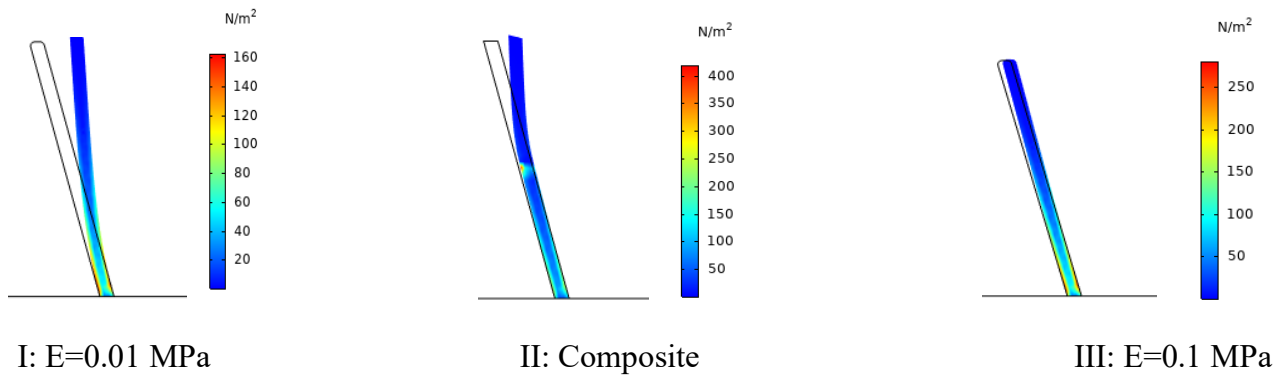


Fig. 7. Stress distributions in the deformed VGs at their equilibrium positions (Zero amplitude)

For the high flexible homogeneous VG ($E=0.01$ MPa), after the initial period, vibration occurs at a lower frequency and higher amplitude based on the flapping mode, as seen in Fig. 6-b. In flow mixing, the number of shedding vortices detached from the trailing edge per unit time decreased due to the decreasing in flapping frequency of soft VG, and the gap distance between the trailing edge and the shedding vortices increased in this case. This behavior leads to less mixing rate in the thermal boundary layer of convection flow.

The time history of displacement for composite VG shown in Fig. 6-c reveals the flapping mode with relatively high amplitude and frequency. It should be noted that the composite VG is made of two distinct parts with relatively soft and hard materials, as shown in Fig. 2. The second part of VG near to its free oscillating tip is made with high elastic material for having large deformation and bending due to FSI, and the lower part is more rigid to have a high frequency. Thereby, it is claimed that that the proposed method can be introduced as an efficient way for more mixing rate and convection enhancement.

In Fig. 7, the deformed shapes of vibrating winglets at their equilibrium positions (zero amplitude) and also the stress distribution inside the VGs are shown. As expected, large deformation occurs in soft homogenous VG because of the FSI, and small deformation occurs in hard one, such that composite VG is placed between them. But, in convection enhancement and flow mixing, the amplitude and frequency of VG oscillation are very important and have the main role. For more study, the values of amplitude and frequency of VGs at their flapping or irregular vibration modes are given in Table. 4. As an important and interesting finding, one can note the high amplitude of composite VG, which is even more than the soft homogeneous winglet, while both of them vibrate with almost equal frequency. So, more mixing rate in convection flow will be expected in using composite VG compared to homogenous ones. About the stress distribution in winglets, the numerical results reveal relatively low and high stresses inside the soft and hard VGs, respectively. But for the composite winglet, Fig. 7-b depicts a thin region at the middle of VG with very high stress due to the Young modulus variation with a large gradient at this zone.

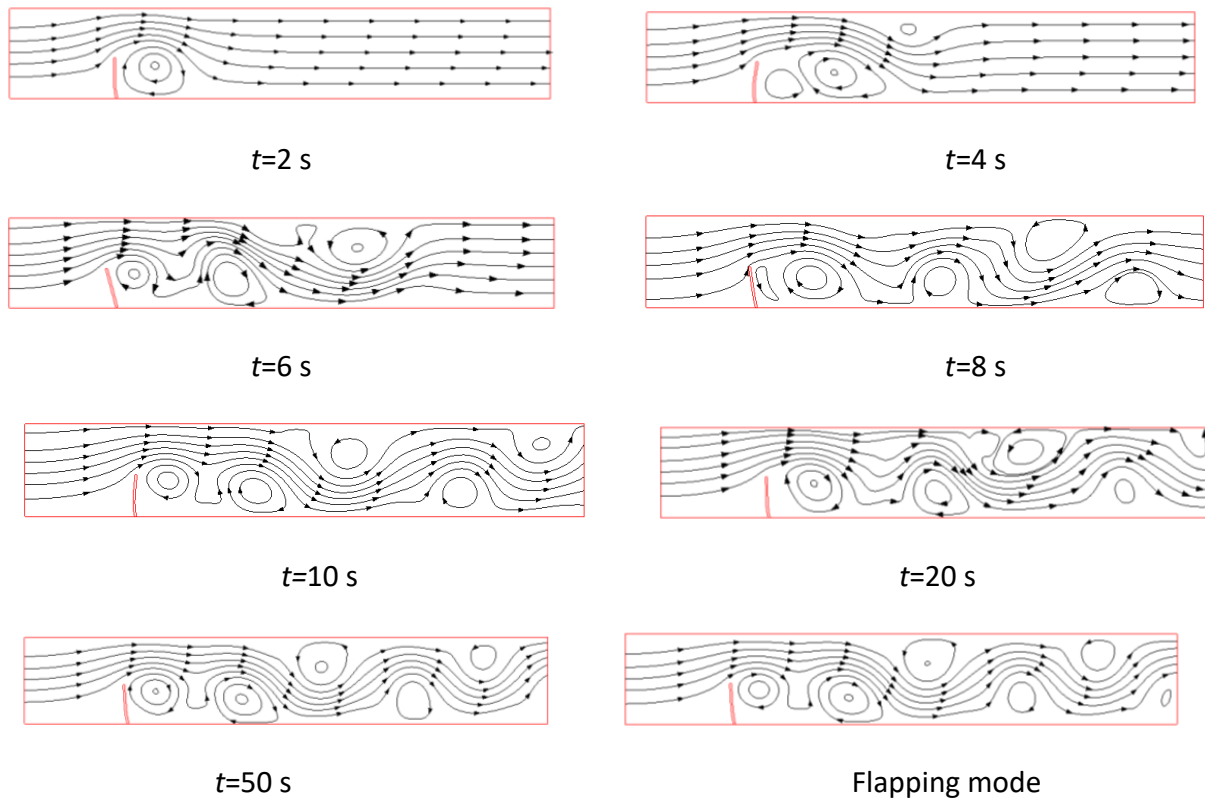


Fig. 8. Streamline plots for laminar convective flow under the presence of composite VG

6-2- Flow and thermal behavior of flowing gas with composite VG

To demonstrate the efficient mixing effect of oscillating composite VG on flow and thermal behavior of convective air flow, the streamline plots inside the channel bounded by two heated fins at different time steps from $t=0$ s to $t=50$ sec are drawn in Fig. 8. Flow vortices due to the vibration of VG are seen at initial times in this figure. These recirculated zones are detached from the winglet and move along the heat sink such that moving arranged rows of vortices are transported toward the outlet section by progressing in time. This phenomenon is known to be responsible for heat transfer enhancement in transient forced convection flow. The vortex shedding process due to the shear layer instability offers an important feature related to the existence of a constructive mode, where the vortices of the same rotating sense merge together, resulting in larger recirculated domains. It should be noted that after $t=50$ s when the vibrating VG reaches its flapping mode, the semi-steady condition is called for the state of the system. For presenting more about the hydrodynamic behavior of convection flow, the contours of velocity magnitude are drawn in Fig. 9. In all captured moments, the moving regions with high local values of air velocity can be recognized due to the VG oscillation. The flow vortices and the related recirculated domains are seen in Fig. 9.

The pressure contours at the flapping mode of oscillation are drawn in Fig. 10. This figure shows the domain with high pressure upstream of the winglet because of the blockage effect. The regions with low pressure inside the flow vortices, which are moving along the flow are also seen in Fig. 10.

Fig. 11 displays the contour of temperature in air convective flow at different times up to a semi-steady state. As seen for all captured moments, the maximum temperature in the gas domain takes place near heated fins, as well as the area inside the recirculated zones downstream of VG. The mixing effect of VG that leads to breaking the thermal boundary layer and enhancing the convection heat transfer is seen in Fig. 11. Because of the periodic oscillations of the flapping vortex generator and the convective air flow through FSI, the temperature field is stirred and the thermal energy transfers from the high temperature boundary surfaces to the core of the convective air flow by progressing in time. The complex pattern of vortex shedding due to the shear layer instability offers an important feature related to the existence of a constructive mode [14], where the vortices of the same rotating sense merge together to form larger eddies as shown in the study by Ali et al. [15]. This process was previously seen in Fig. 8, such that vortex pairing produces vortices of higher strength in the air flow. This is an essential criterion to disrupt the growth of the thermal boundary layer and carry the hot air near the heated wall to mix with the core of cold air flow

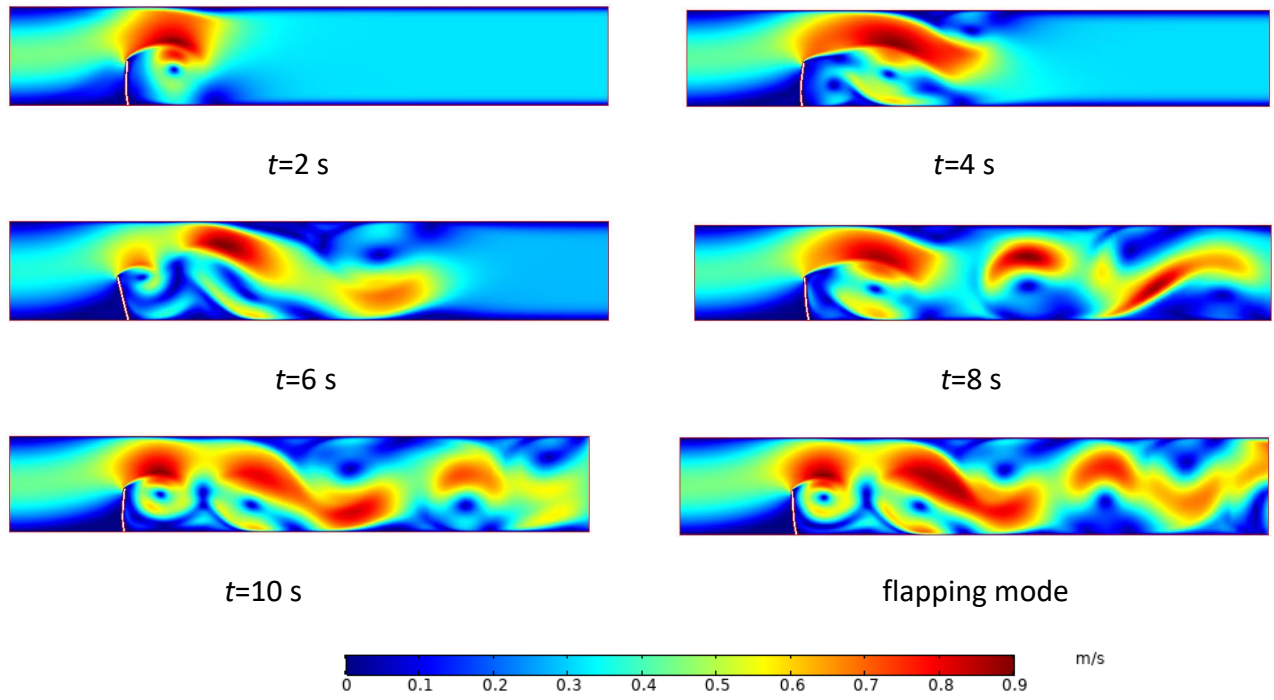


Fig. 9. Velocity magnitude contours

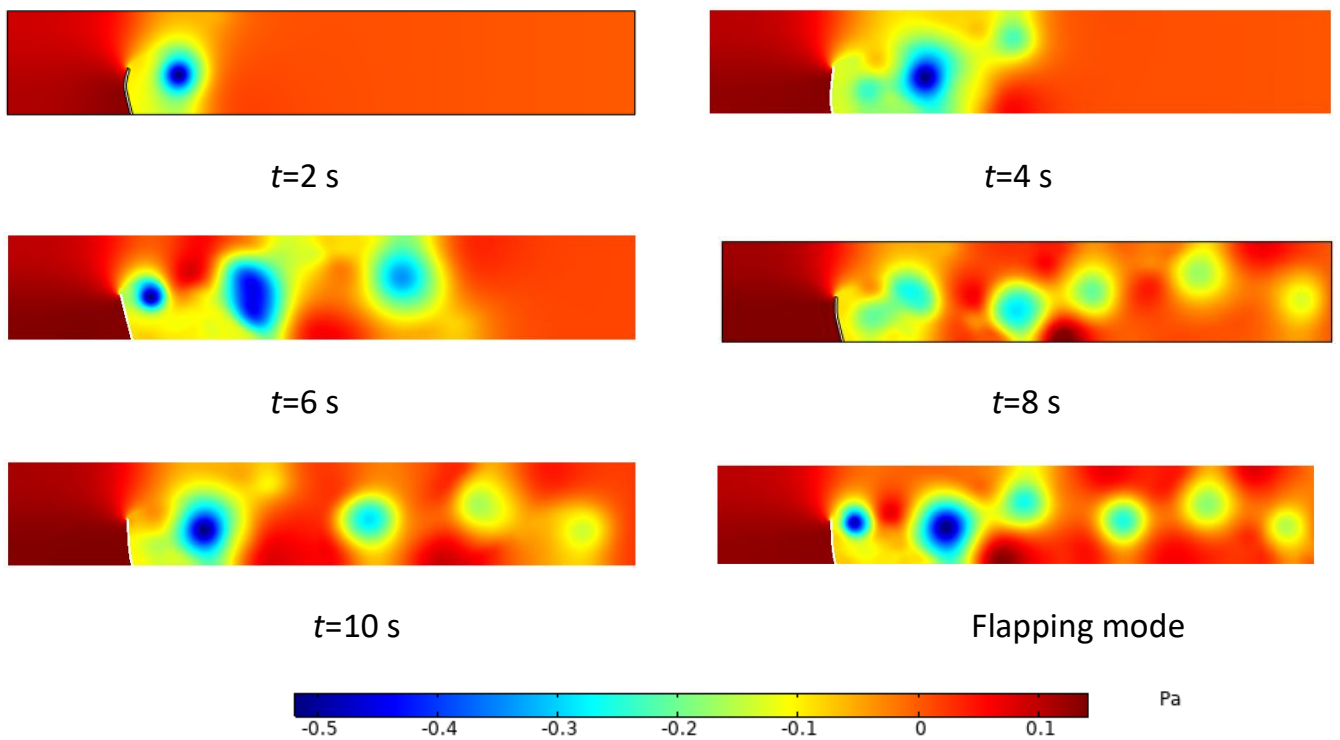


Fig. 10. Pressure contours at different times

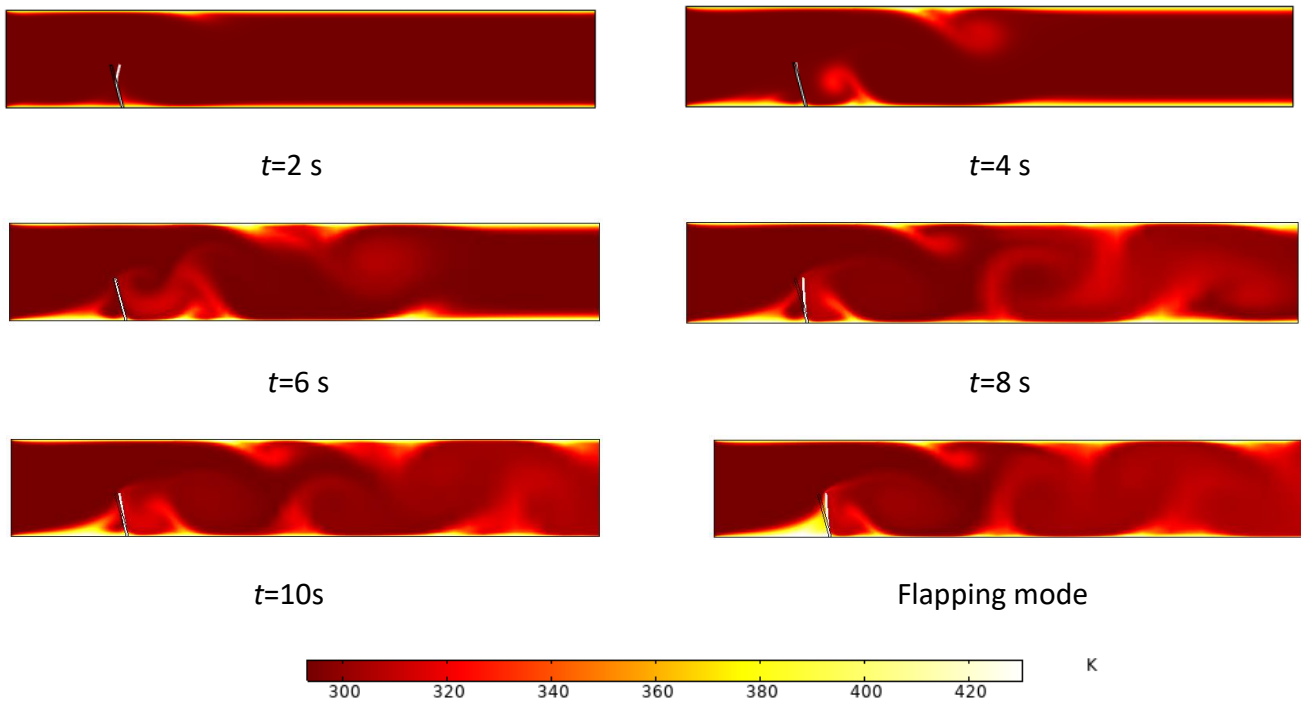


Fig. 11. Temperature contours

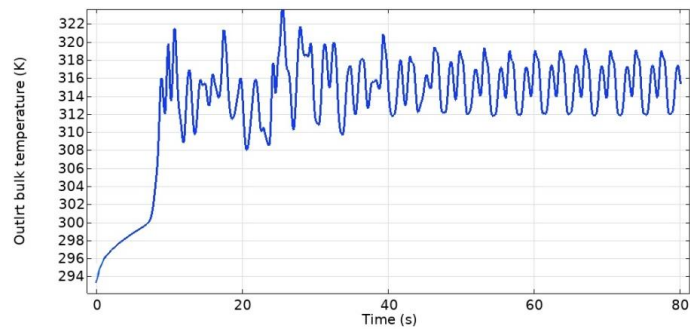
at the centerline of the heat sink. This process is enhanced at the flapping mode of oscillation due to the VG vibration with high frequency and large amplitude, compared to the two irregular and fully deflected modes.

To demonstrate the preference of using composite VG, the time history of air outlet temperature from the simulated heat sink for all of the test cases, including the clean duct (without VG), are presented in Fig. 12. Since the numerical results have shown the flapping or irregular mode of oscillation for the VGs, the same trend is also seen for the gas outlet temperature because of the flow vortices and moving recirculated domains in the gas convection flow. The time average values of outlet air temperature during a full period in semi-steady conditions are also computed and are mentioned in each figure caption. If the clean duct is considered as the base case, equal to 148%, 121%, and 116% increases in the rate of convection heat transfer $q = \dot{m}c_p (T_{m\ out} - T_{in})$ can be computed for the composite and two homogeneous VGs, respectively. Such that for homogeneous winglets, the soft one operates relatively better in convection enhancement.

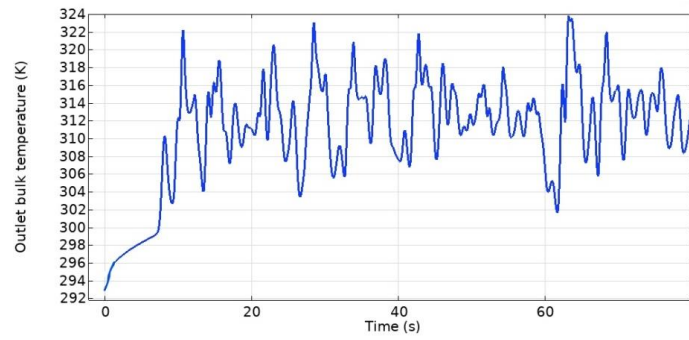
Finally, the contours of velocity magnitude and temperature for the case of clean duct are plotted in Fig. 13 for having

a better image of vortex generation technique in flow mixing and convection enhancement. As seen in Fig. 13-a, the working fluid enters into the duct with a fully developed velocity profile. Due to the no-slip condition, the air velocity maintains this pattern along the duct with a slight increase in velocity inside the heated region near the hot boundaries where the air density is decreased due to its dependence on temperature. In Fig. 13-b, it is seen that only the two thin layers adjacent to the top and bottom hot walls are heated effectively and the thermal energy is not permitted to penetrate into the core of convection flow. This poor ability of clean duct convection flow for the heat sink cooling is due to the low value of air thermal conduction, especially in the absence of flow vortices and the mixing process. This behavior leads to a small value of Nusselt number along the heated wall as shown in Fig. 14.

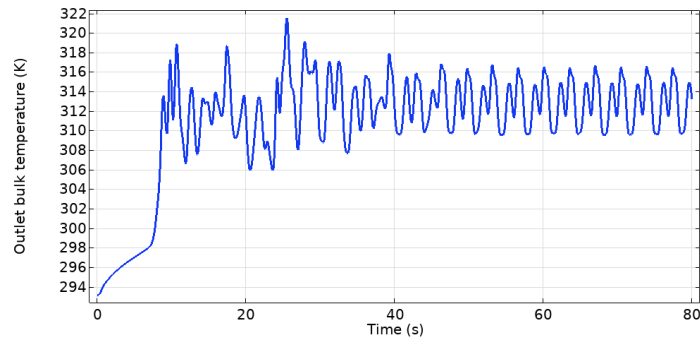
At the end of the result section, it should be recalled that the advantage of composite vortex generators in convection enhancement was also seen along with several other test cases with different Reynolds numbers and thermal conditions, but the related results are not reported in this paper for space-saving.



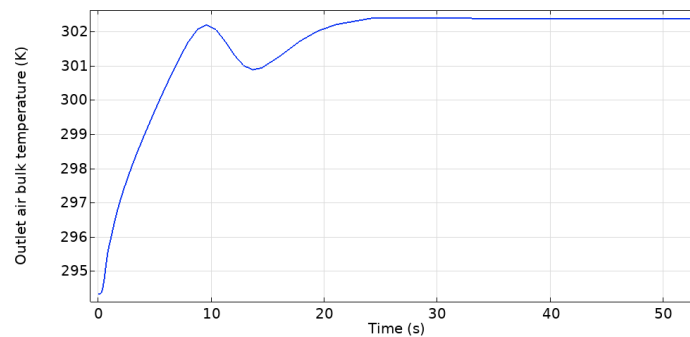
a) Composite VG at flapping mode ($\bar{T}_{m out} = 316.1$ K)



b) $E=0.1$ MPa at irregular mode ($\bar{T}_{m out} = 313.1$ K)



c) $E=0.01$ MPa at flapping mode ($\bar{T}_{m out} = 313.6$ K)



d) Without VG ($\bar{T}_{m out} = 302.4$ K)

Fig. 12. Time history of air outlet temperature

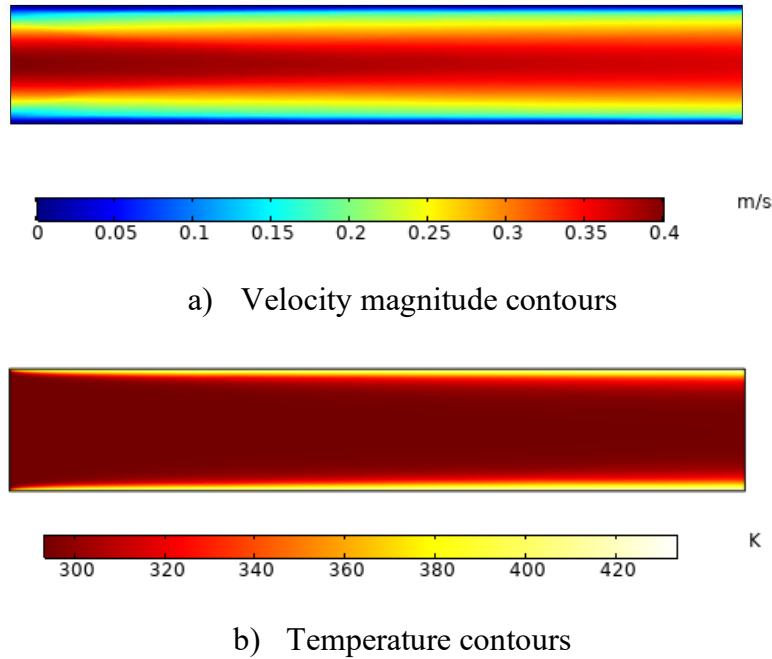


Fig. 13. Velocity magnitude and temperature contours of convection flow in the clean duct at a steady state.

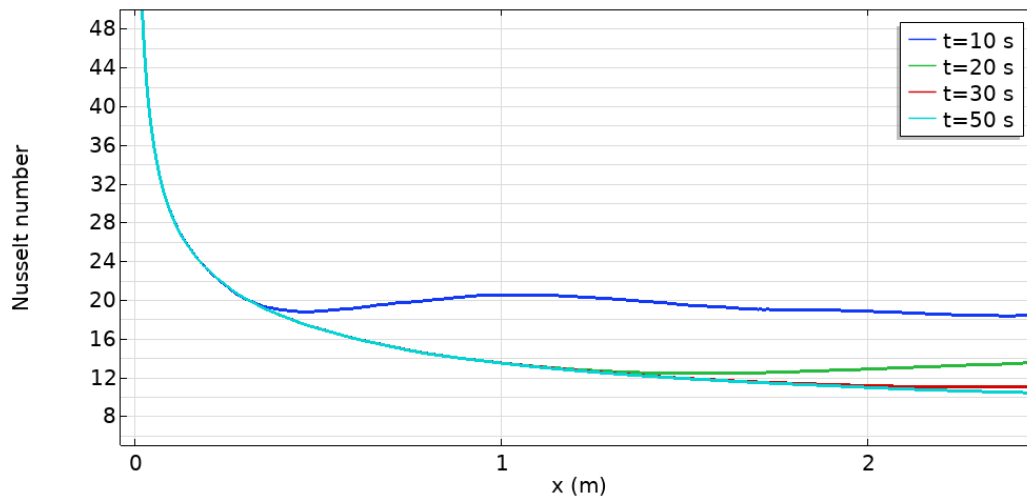


Fig. 14. Variation of Nusselt number along the heated wall at different times

7- Conclusion

This study was dedicated to the sustainable solution for exploiting high-performance heat sinks by proposing a new idea of employing composite vortex generators for convection enhancement. In the numerical simulation, the set of governing equations including the conservations of mass, momentum, and energy for laminar forced convection air flow coupled with fluid-solid interaction was solved in transient condition by the FEM. The main results can be summarized as follows:

- The vortex generation technique enhances the convection heat transfer by introducing the flow vortices that swept

out the thermal boundary layer and causes thermal mixing in the wake.

- Numerical findings reveal a large amplitude in the oscillation of the composite VG at the flapping mode, even more than the soft winglet under the same flow condition.

- The developing composite vortex generator can improve the rate of heat rejection by 148%, while the improvements in the cases of using soft and hard homogeneous VGs are 121% and 116%, respectively, compared with the clean heat sink.

Nomenclature

c_p	Specific heat (J/kg K)	Gree
D_h	Hydraulic diameter (m)	
F	Force per unit volume (N/m ³)	
h	Convection coefficient (W/m ² K)	
k	Thermal conductivity (Wm ⁻¹ K ⁻¹)	
L	Length (m)	
\dot{m}	Mass flow rate (kg/s)	
p	Pressure (Pa)	
q	Rate of heat transfer (W)	
Re	Reynolds number	St
t	Time (s)	
T	Temperature (K)	
$U_{s,i}$	Displacement vector (m)	
(x, y)	Cartesian coordinate (m)	
(u, v)	Velocity components (m/s)	
V	Velocity magnitude (m)	

Greek symbols

α	Thermal diffusivity (m ² /s)
β	Attacked angle
μ_s	Lame's second parameter (Pa)
μ	Dynamic viscosity (Pa.s)
ν	Poisson ratio
ρ	Density (kg/m ³)
λ	Lame's first parameter (Pa)

Subscript

i, j	Indices
in	Inlet
m	Mean bulk
out	Outlet
s	Solid
w	Wall

References

- [1] A. Beskok, M. Raisee, B. Celik, B. Yagiz, M. Cheraghi, Heat transfer enhancement in a straight channel via a rotationally oscillating adiabatic cylinder, *International Journal of Thermal Sciences*, 58 (2012) 61-69.
- [2] J. Shi, J. Hu, S.R. Schafer, C.-L. Chen, Numerical study of heat transfer enhancement of channel via vortex-induced vibration, *Applied Thermal Engineering*, 70(1) (2014) 838-845.
- [3] J.S. Go, Design of a microfin array heat sink using flow-induced vibration to enhance the heat transfer in the laminar flow regime, *Sensors and Actuators A: Physical*, 105(2) (2003) 201-210.
- [4] C.B. Allison, B.B. Dally, Effect of a delta-winglet vortex pair on the performance of a tube-fin heat exchanger, *International Journal of Heat and Mass Transfer*, 50(25) (2007) 5065-5072.
- [5] S. Ali, C. Habchi, S. Menanteau, T. Lemenand, J.-L. Harion, Three-dimensional numerical study of heat transfer and mixing enhancement in a circular pipe using self-sustained oscillating flexible vorticity generators, *Chemical Engineering Science*, 162 (2017) 152-174.
- [6] Z. Li, X. Xu, K. Li, Y. Chen, G. Huang, C.-I. Chen, C.-H. Chen, A flapping vortex generator for heat transfer enhancement in a rectangular airside fin, *International Journal of Heat and Mass Transfer*, 118 (2018) 1340-1356.
- [7] S. Ali, S. Menanteau, C. Habchi, T. Lemenand, J.-L. Harion, Heat transfer and mixing enhancement by using multiple freely oscillating flexible vortex generators, *Applied Thermal Engineering*, 105 (2016) 276-289.
- [8] R.K.B. Gallegos, R.N. Sharma, Heat transfer performance of flag vortex generators in rectangular channels, *International Journal of Thermal Sciences*, 137 (2019) 26-44.
- [9] J.B. Lee, S.G. Park, B. Kim, J. Ryu, H.J. Sung, Heat transfer enhancement by flexible flags clamped vertically in a Poiseuille channel flow, *International Journal of Heat and Mass Transfer*, 107 (2017) 391-402.
- [10] S.G. Park, Heat transfer enhancement by a wall-mounted flexible vortex generator with an inclination angle, *International Journal of Heat and Mass Transfer*, 148 (2020) 119053.
- [11] P. Le Tallec, J. Mouro, Fluid structure interaction with large structural displacements, *Computer Methods in Applied Mechanics and Engineering*, 190(24) (2001) 3039-3067.
- [12] W.B. Zimmerman, *Multiphysics modeling with finite element methods*, World Scientific Publishing Company, 2006.
- [13] O.C. Zienkiewicz, R.L. Taylor, P. Nithiarasu, J. Zhu, *The finite element method*, McGraw-hill London, 1977.
- [14] R. Gopalkrishnan, M.S. Triantafyllou, G.S. Triantafyllou, D. Barrett, Active vorticity control in a shear flow using a flapping foil, *Journal of Fluid Mechanics*, 274 (1994) 1-21.
- [15] S. Ali, C. Habchi, T. Lemenand, J.-L. Harion, Towards self-sustained oscillations of multiple flexible vortex generators, *Fluid Dynamics Research*, 51(2) (2019) 025507.

HOW TO CITE THIS ARTICLE

S. A. Gandjalikhan Nassab, M. Moein Addini, *Convection Enhancement Using Composite Vortex Generator*, *AUT J. Mech Eng.*, 6 (1) (2022) 149-164.

DOI: [10.22060/ajme.2021.20158.5992](https://doi.org/10.22060/ajme.2021.20158.5992)



